



# Estimation of optical model parameters and their correlation matrix using Unscented Transform Kalman Filter technique



Aman Sharma, A. Gandhi, Ajay Kumar\*

Department of Physics, Banaras Hindu University, Varanasi 221005, India

## ARTICLE INFO

### Article history:

Received 3 December 2020  
Received in revised form 22 February 2021  
Accepted 22 February 2021  
Available online 24 February 2021  
Editor: W. Haxton

### Keywords:

Optical model parameters  
Unscented Transform Kalman Filter  
Uncertainty quantification and TALYS

## ABSTRACT

In the present study, we have optimized the optical model parameters and also calculated their correlation matrix using the Unscented Transform Kalman Filter technique for the first time. We have used  $n+^{56}\text{Fe}$ ,  $n+^{45}\text{Sc}$  and  $n+^{59}\text{Co}$  reactions for this study in order to verify the application of this method. We have used the experimental differential cross section data for the elastically scattered neutrons from the EXFOR data library and DWBA calculations to determine the parameters. In this study we have assumed that the optical model provides correct results and the uncertainties come from the variation of fitting parameters only. We have used the TALYS nuclear reaction code for the DWBA calculations. The optical model parameters determined through this study, reproduce the calculations which are consistent with the experimental trends for the elastically scattered neutrons and total reaction cross sections. Also the correlations calculated in this work are consistent with the earlier study of  $n+^{56}\text{Fe}$  reaction.

© 2021 The Author(s). Published by Elsevier B.V. This is an open access article under the CC BY license (<http://creativecommons.org/licenses/by/4.0/>). Funded by SCOAP<sup>3</sup>.

## 1. Introduction

A good quality nuclear reaction data over a wide range of the projectile energy is one of the primary ingredients for the development of the future nuclear technologies. But the direct measurements of nuclear reactions are not possible for all the projectile energies and all the target mass range, because of the practical issues like projectile energy resolution, stable target availability etc. In such kind of situation, one has to rely more on the theoretical predictions for producing the evaluated nuclear data files like ENDF/B-VII.1, CENDL-3.1 and JENDL-4.0 etc. Nowadays, more importance is being given to the better estimation of nuclear data uncertainties and covariance, as these are of high importance for calculating the uncertainties in the design parameters of the nuclear facilities.

There are number of nuclear reaction models which are used to predict and interpret the experimental data. These models use set of parameters, which are normally determined by comparing the model predictions with the available experimental data. Hence the quality of these parameters will affect the quality of the model predictions. Information about the uncertainties and correlations between these model parameters is also important. These un-

tainties of the parameters can be used to estimate the uncertainties and covariance matrix associated with the model predictions using Total Monte Carlo (TMC) method [1]. Few efforts in this direction have been made since the past decade, and some information about the model parameters uncertainties along with their correlations have also been included in the RIPL-3 library [2]. It uses Monte Carlo method for producing these estimations, but this study is in its early stage, and the provided estimates are proof of the principle only, which means there is enough room to explore and discuss other methods. The uncertainty quantification of the model parameters is also very important from the perspective of the nuclear reaction theory as it provides a deep understanding about the uncertainties within the models [3].

There are different techniques used in the literature for the parameter estimation and uncertainty quantification, e.g. Extended Kalman Filter [4],  $\chi^2$  minimization [3,5], Monte Carlo techniques [6] etc. The EMPIRE-KALMAN approach [4] used for the parameter correlation estimation and optimization uses the extended Kalman filter technique (EKFT). Hence it is required to calculate the partial derivatives of the model with respect to all the parameters i.e. sensitivity matrix. This is a cumbersome process and also approximates the uncertainties only up to the first order of the Taylor series expansion. In an another study correlated and uncorrelated  $\chi^2$  minimization functions have been used to calculate the correlations between the optical model parameters [3]. But this method also requires to calculate the Jacobian matrix of model functions with respect to the parameters, hence has the limitations similar

\* Corresponding author.

E-mail addresses: [aman.marley1314@gmail.com](mailto:aman.marley1314@gmail.com) (A. Sharma), [ajaytayagi@bhu.ac.in](mailto:ajaytayagi@bhu.ac.in) (A. Kumar).

to the EKFT. A completely different approach by Duan et al., [6] based on the Monte Carlo method uses random sampling of the parameters from a Gaussian distribution and then uses accept and reject approach to produce the updated estimate of the parameters and their covariance matrix. But this method takes long time and large computational power as compared to the EMPIRE-KALMAN approach.

In the present study, we have used the Unscented Transform Kalman filter (UTKF) technique for the estimation of the optical model parameters and their uncertainties. This method eliminates the difficulties associated with the EKFT and the  $\chi^2$  minimization techniques, because in this method we do not have to calculate the Jacobian matrix and also it approximates the uncertainties at least up to the second order of the Taylor series expansion. Moreover this method requires very few calculations as compared to the Monte Carlo technique. The optical model potential provides an invaluable tool for calculating the elastic, inelastic and total reaction cross sections. The optical model parameters are generally optimized by fitting the model predictions with the experimental elastic and inelastic scattering data. It had been known that some of these parameters are strongly correlated and can have high uncertainties [6,7]. The unscented transform was firstly introduced by Uhlmann and Julier [8–10], and was adopted for improving estimates provided by the extended Kalman filter. Since then this method is rapidly replacing the extended Kalman filter in various fields of engineering and computer science [11,12]. The UTKF does not use partial derivatives, but rather uses carefully chosen points assuming the probability distribution of the parameters is Gaussian to propagate the uncertainties. In the Unscented Transform method a set of sigma points is obtained deterministically in such a way that their mean and covariance matches the probability distribution of the input parameters. Also when these sigma points are propagated through the nonlinear functions, the ensemble of output sigma points contain the information about the mean and covariance of the output. This method is based on the assumption that it is easier to approximate a probability distribution than to approximate an arbitrary nonlinear function. Higher order information about the distribution can be captured using only very small number of points, hence uses small number of calculations as compared to the Monte Carlo method.

The objective of this study is to establish the fact that the UTKF technique can be used for the uncertainty quantification of the optical model parameters. We have calculated the optical model parameters for  $n+^{56}\text{Fe}$ ,  $n+^{45}\text{Sc}$  and  $n+^{59}\text{Co}$  reactions using the UTKF technique. In section 2 we have discussed the optical model potential used in the present study. In section 3, the formulation of the UTKF technique used for the parameter estimation has been described. Section 4 describes the methodology of the present study; results and conclusions are presented in section 5 and 6, respectively.

## 2. Optical model potential

In this manuscript, we have used the Wood-Saxon phenomenological optical model potential. This form of the potential has been used extensively in the past studies [5,13]. The phenomenological optical model potential for the interaction of neutron and nucleus is generally given as:

$$\begin{aligned} \mathcal{U}(r, E) = & -\mathcal{V}_V(r, E) - i\mathcal{W}_V(r, E) - i\mathcal{W}_D(r, E) + \\ & \mathcal{V}_{SO}(r, E).1.\sigma + i\mathcal{W}_{SO}(r, E).1.\sigma \end{aligned} \quad (1)$$

Here  $\mathcal{V}$ 's represent the real part while  $\mathcal{W}$ 's represent the imaginary part of the different potentials (i.e. volume central (V), surface central (D) and spin orbit (SO)). We can separate the potentials in

terms of the incident energy (E) dependent and independent parts as given below.

$$\mathcal{V}_V(r, E) = V_V(E)f(r, R_V, a_V) \quad (2)$$

$$\mathcal{W}_V(r, E) = W_V(E)f(r, R_V, a_V) \quad (3)$$

$$\mathcal{W}_D(r, E) = -4a_D W_D(E) \frac{d}{dr} f(r, R_D, a_D) \quad (4)$$

$$\mathcal{V}_{SO}(r, E) = V_{SO}(E) \left( \frac{\hbar}{m_\pi c} \right)^2 \frac{1}{r} \frac{d}{dr} f(r, R_{SO}, a_{SO}) \quad (5)$$

$$\mathcal{W}_{SO}(r, E) = W_{SO}(E) \left( \frac{\hbar}{m_\pi c} \right)^2 \frac{1}{r} \frac{d}{dr} f(r, R_{SO}, a_{SO}) \quad (6)$$

Here the energy independent form factor  $f(r, R_i, a_i)$  is having Woods-Saxon shape.

$$f(r, R_i, a_i) = (1 + \exp[(r - R_i)/a_i])^{-1} \quad (7)$$

Where  $r_i$  and  $a_i$  are assumed as constants, independent of the energy and can be determined by comparing the model predictions with the experimental results. We have used  $(E - E_f)$  dependent functional forms for the present study as presented below and  $E_f$  is the Fermi energy in MeV.

$$V_V(E) = v_1 \left[ 1 - v_2(E - E_f) + v_3(E - E_f)^2 - v_4(E - E_f)^3 \right] \quad (8)$$

$$W_V(E) = w_1 \frac{(E - E_f)^2}{(E - E_f)^2 + (w_2)^2} \quad (9)$$

$$W_D(E) = d_1 \frac{(E - E_f)^2}{(E - E_f)^2 + (d_3)^2} \exp[-d_2(E - E_f)] \quad (10)$$

$$V_{SO}(E) = v_{so1} \exp[-v_{so2}(E - E_f)] \quad (11)$$

$$W_{SO}(E) = w_{so1} \frac{(E - E_f)^2}{(E - E_f)^2 + (w_{so2})^2} \quad (12)$$

$v_1, v_2, v_3, v_4, w_1, w_2, d_1, d_2, d_3, v_{so1}, v_{so2}, w_{so1}$  and  $w_{so2}$  are the fitting parameters and can be estimated by fitting the model predictions to the experimental data.

## 3. Parameter estimation using the Unscented Transform Kalman Filter

The unscented transform Kalman filter is a powerful tool for the parameter and state estimation. The detailed derivation and the applications of the UTKF technique are well documented and the technical details can be found in ref. [9,12,14,15]. Here we have briefly described the process of the parameter estimation for a problem in hand. Consider we have a large number of  $N$  dimensional vectors of the experimental measurements ( $d$ ) and a prior estimate of the parameter vector ( $\theta_0$ ) of dimension  $L$  and their covariance matrix  $P_0$ . Let  $G(\theta_k)$  is a model and the experimental results have to be compared with this model. Here the index  $k$  represents the calculations for the  $k^{th}$  experimental data set ( $k \in 1, 2, 3, \dots, \infty$ ). We can write the time update equations for estimating the parameters for  $k^{th}$  experimental data set as  $\theta_k^- = \theta_{k-1}$  and  $P_{\theta_k}^- = P_{k-1} + R_{k-1}^r$  [12]. Here  $R^r$  represents the process noise covariance and there are different options available to choose  $R^r$  in the literature [12]. For  $\theta_k^-$  and  $P_{\theta_k}^-$  we can generate a  $L \times (2L + 1)$  dimensional matrix ( $W$ ) containing  $(2L + 1)$  sets of the sigma points using the unscented transform as given below.

$$W_{k|k-1} = \left[ \theta_k^- \quad \theta_k^- + \sqrt{(L + \lambda)P_{\theta_k}^-} \quad \theta_k^- - \sqrt{(L + \lambda)P_{\theta_k}^-} \right] \quad (13)$$

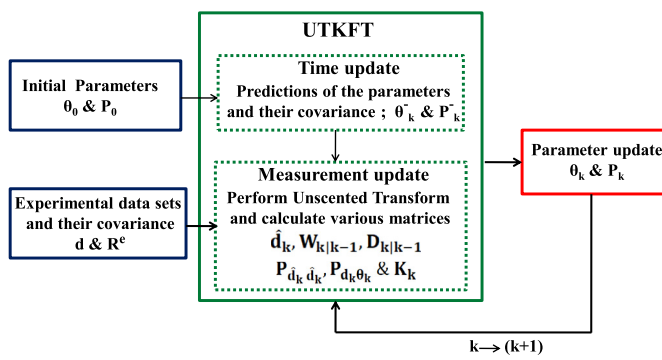


Fig. 1. Flow chart for UTKF technique calculation for the present work.

The matrix square root ( $\sqrt{(L + \lambda)P_{\theta_k}}$ ) can be calculated using various numerically stable methods and here we have used the Cholesky decomposition method [16]. The corresponding weights to these sigma points are given in the following equations, where the superscripts (m) and (c) indicate that these weights should be used while calculating the mean and the covariances respectively.

$$w_0^{(m)} = \lambda/L + \lambda \quad (14)$$

$$w_0^{(c)} = \lambda/(L + \lambda) + (1 - \alpha^2 + \beta) \quad (15)$$

$$w_i^{(m)} = w_i^{(c)} = 1/2(L + \lambda); \quad i = 1, 2, \dots, 2L \quad (16)$$

The constants  $\alpha$ ,  $\kappa$  and  $\beta$  are the scaling parameters used to approximate the probability distribution function of the input parameters, while  $\lambda = \alpha^2(L + \kappa) - L$ . For the present study we have used  $\kappa = 3 - L$  [10];  $\beta = 2$  and  $1 \geq \alpha \geq 10^{-4}$  [17].

Using  $(2L + 1)$  sets of the parameters i.e. sigma points, we can generate a  $N \times (2L + 1)$  dimensional matrix ( $D$ ) containing  $(2L + 1)$  sets of model predictions using the model function  $G(\theta_k)$ . From this ensemble of model predictions we can calculate mean ( $\hat{d}_k$ ) and a covariance matrix of the measurement estimates [10]. We have also added the experimental covariance matrix ( $R_k^e$ ) to the covariance matrix of the measurement estimates to define the final covariance matrix ( $P_{\hat{d}_k \hat{d}_k}$ ) of the measurement estimates. We can calculate the cross covariance matrix ( $P_{d_k \theta_k}$ ) between the parameters and the measurement estimates by using the  $W$  and  $D$  matrices [15]. We can also calculate the Kalman gain ( $K_k = P_{d_k \theta_k} P_{\hat{d}_k \hat{d}_k}^{-1}$ ) using the covariance ( $P_{\hat{d}_k \hat{d}_k}$ ) and the cross covariance ( $P_{d_k \theta_k}$ ) matrices. Finally the updated parameters and their covariance matrix are calculated as:

$$\theta_k = \theta_k^- + K_k(d_k - \hat{d}_k) \quad (17)$$

$$P_{\theta_k} = P_{\theta_k}^- - K_k P_{\hat{d}_k \hat{d}_k} K_k^T \quad (18)$$

Now for the next set of the experimental measurements i.e. for  $(k + 1)^{th}$  set, these updated parameters and their covariance matrix are considered as a prior estimation and the whole process is repeated again to further update the parameters. A flow chart describing the calculation process as mentioned above has been presented in Fig. 1.

#### 4. Methodology

In order to determine the optical model potential parameters and their uncertainties for the reactions  $n + {}^{56}\text{Fe}$ ,  $n + {}^{45}\text{Sc}$  and  $n + {}^{59}\text{Co}$ , the DWBA calculations of the differential cross sections for the elastically scattered neutrons were compared with the experimental data from EXFOR data library [18] using the UTKF algorithm. DWBA calculations were carried out using the TALYS nuclear

reaction code [19]. We have determined 18 optical model parameters in this work which are listed in column 1 of Table 1. We have also used the global optical model parameters of Koning and Delaroche [13] as our initial estimate of the parameters, and an initial estimate of the uncertainties of these parameters was used from ref. [7]. The unscented transform method was used to generate the sigma points ( $2 \times 18 + 1 = 37$  set of parameters). The angular distribution of the elastic spectra of neutrons corresponding to each set of the parameters was calculated using the DWBA analysis through the TALYS nuclear reaction code and consequently an ensemble of thirty-seven outputs of the angular distribution was created. We have calculated the Kalman gain, covariance matrix and cross-covariance matrix of this ensemble. Also we have calculated an updated estimate of the parameters and their covariance matrix using equation (17) and (18). In order to incorporate the correlations between the differential cross section data at different energies, we have combined all the experimental data at different incident energies for a particular reaction into one set. Since there was not sufficient information about the covariance of the experimental data in the EXFOR, therefore a diagonal matrix with the square of the experimental uncertainties was created for the calculations. We have used default values of the level densities and other necessary parameters in TALYS for the compound nucleus contribution; however such contributions were very low as compared to the direct channel. We have calculated the average  $\chi^2$  value for the model prediction with initial parameters and final parameters, for comparison with the experimental data.

$$\chi^2 = \frac{1}{N} \sum_{i=0}^N \left( \frac{\sigma_T^i - \sigma_E^i}{\Delta \sigma_E^i} \right)^2 \quad (19)$$

Where  $N$  is the total number of the experimental data points used for a particular reaction. A MatLab script was written to perform all these calculations.

We have used the experimental differential elastic scattering data of S. M. El-Kadi et al., [20] and A. P. D. Ramirez et al., [21], for  $n + {}^{56}\text{Fe}$  reaction. They have measured the angular distribution of the elastically scattered neutron from  $30^\circ$  to  $160^\circ$  in the lab frame for the neutron energies ranging from 1 to 14 MeV. The experimental differential cross sections for the elastically scattered neutrons for  $n + {}^{45}\text{Sc}$  reaction have been used from A. B. Smith et al., [22] for determining the optical model parameters. They have measured the spectra of the elastically scattered neutrons from  $15^\circ$  to  $160^\circ$  in the lab frame for neutron energies from 1 to 9 MeV. The experimental data of A. B. Smith et al., [23] was used for determining the optical model parameters for the reaction  $n + {}^{59}\text{Co}$ . They have measured the angular distribution of the elastically scattered neutrons from  $20^\circ$  to  $160^\circ$  in the lab frame for neutron energies from 1 to 14 MeV. The angular distribution calculated using the global optical model parameters (initial parameters) and parameters calculated through this study is presented in Fig. 2, 4 and 6. The correlation matrix of the parameters calculated in the present study is displayed in Fig. 3, 5 and 7. We have used the optical model parameters obtained in this study to predict the total reaction cross sections of these three reactions, as shown in Fig. 8.

#### 5. Results

The differential cross sections for the elastically scattered neutrons calculated using initial and new set of the optical model parameters have been presented in Fig. 2, 4 and 6 in comparison with the experimental data used in this study. It is clear from the figures that the new set of the optical model parameters presents

**Table 1**

Comparison of the initial and updated set of the optical model parameters and the associated percentage uncertainties given in the parentheses, for different reactions studied in this work.  $a_v$ ,  $r_v$ ,  $a_d$ ,  $r_d$ ,  $a_{so}$  and  $r_{so}$  are in fm;  $v_1$ ,  $d_1$ ,  $d_3$ ,  $w_1$ ,  $w_2$ ,  $w_{so1}$ ,  $w_{so2}$  and  $v_{so1}$  are in MeV;  $d_2$ ,  $v_{so2}$ ,  $v_2$  are in  $\text{MeV}^{-1}$  and  $v_3$  in  $\text{MeV}^{-2}$ .

Parameters S.No.	Parameters for $n+^{56}\text{Fe}$		Parameters for $n+^{45}\text{Sc}$		Parameters for $n+^{59}\text{Co}$		
	Initial	Updated	Initial	Updated	Initial	Updated	
1	$r_v$	1.198(2)	1.212(0.62)	1.190(2)	1.243(0.66)	1.200(2)	1.234(0.63)
2	$a_v$	0.669(2)	0.675(1.05)	0.671(2)	0.673(1.00)	0.669(2)	0.673(1.24)
3	$v_1$	56.456(2)	54.731(1.04)	56.820(2)	53.872(1.07)	56.104(2)	52.419(1.00)
4	$v_2$	0.0071(3)	0.0074(2.41)	0.0072(3)	0.0074(2.69)	0.0071(3)	0.0069(2.93)
5	$v_3$	0.000019(3)	0.000019(3.01)	0.000019(3)	0.000019(3.01)	0.000019(3)	0.000019(2.99)
6	$w_1$	13.13(10)	13.50(9.23)	12.95(10)	12.67(9.99)	13.18(10)	11.22(11.57)
7	$w_2$	78.00(10)	72.91(8.74)	77.13(10)	80.69(8.75)	78.24(10)	99.94(7.35)
8	$r_d$	1.338(3)	1.257(0.50)	1.338(3)	1.367(0.52)	1.338(3)	1.252(0.68)
9	$a_d$	0.535(4)	0.531(2.77)	0.537(4)	0.469(3.13)	0.535(4)	0.540(2.75)
10	$d_1$	14.86(10)	15.17(6.06)	14.93(10)	13.81(6.90)	14.64(10)	11.82(7.85)
11	$d_2$	0.0218(10)	0.0248(7.40)	0.0218(10)	0.0225(8.64)	0.0218(10)	0.0302(6.57)
12	$d_3$	11.50(10)	7.60(8.98)	11.50(10)	13.34(5.16)	11.50(10)	2.90(23.31)
13	$r_{so}$	1.016(10)	1.119(2.23)	1.004(10)	0.782(4.89)	1.019(10)	1.161(5.12)
14	$a_{so}$	0.590(10)	0.612(7.82)	0.590(10)	0.531(9.49)	0.590(10)	0.688(7.51)
15	$v_{so1}$	6.09(5)	6.95(2.53)	6.06(5)	6.96(2.98)	6.10(5)	6.40(2.74)
16	$v_{so2}$	0.0040(10)	0.0039(10.26)	0.0040(10)	0.0038(10.46)	0.0040(10)	0.0040(10.05)
17	$w_{so1}$	-3.1(20)	-3.1(20.13)	-3.1(20)	-3.1(20.11)	-3.1(20)	-3.1(20.05)
18	$w_{so2}$	160(20)	78.227(36.58)	160(20)	202.410(14.46)	160(20)	150.290(19.74)

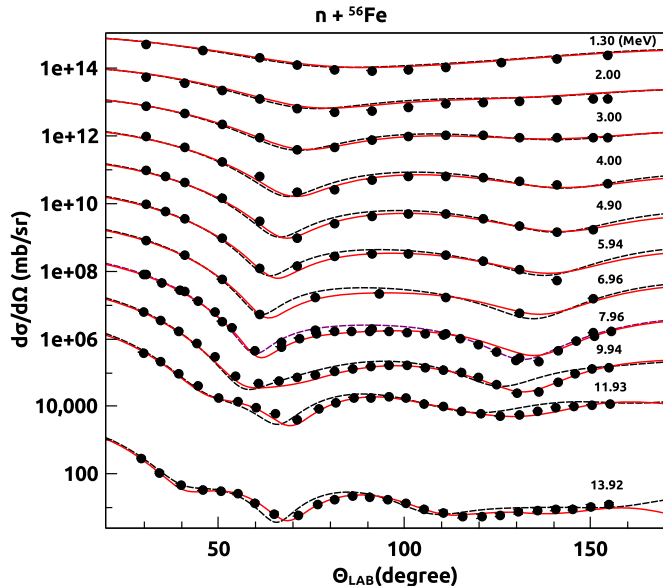


**Fig. 2.** DWBA calculations using updated parameters (in red) relative to the DWBA calculations using initial parameters (in black dotted line) with experimental data (presented in the black dots). Data at different energies have been offset by  $\times 10^3$ ,  $\times 10^4$ ,  $\times 10^5$ ... etc.

a better visual fit to the experimental data as compared to the initial set of parameters. We have calculated average  $\chi^2$  values for our model predictions in order to have an idea about the goodness of the fit. The new set of the optical model parameters have clearly minimized the average  $\chi^2$  value. The average  $\chi^2$  value for  $n+^{56}\text{Fe}$  reaction was 11.683 with initial set of parameters, while 4.796 with the new set of parameters. The value of average  $\chi^2$  was 15.990 with initial parameters and 5.018 with the new parameters for  $n+^{45}\text{Sc}$  reaction. Similarly for  $n+^{59}\text{Co}$  reaction the average  $\chi^2$  was 9.350 with the initial set of parameters, while 3.238 with the updated set of parameters. Since we have used the physically meaningful initial set of parameters [13] and an educated guess of their uncertainties [7]; therefore new set of parameters does not differ much from the initial ones; hence the new set of parameters also represents a set of physically meaningful parameters. The correlation matrices of the new set of the optical model parameters have been presented in Fig. 3, 5 and 7. One can clearly observe that

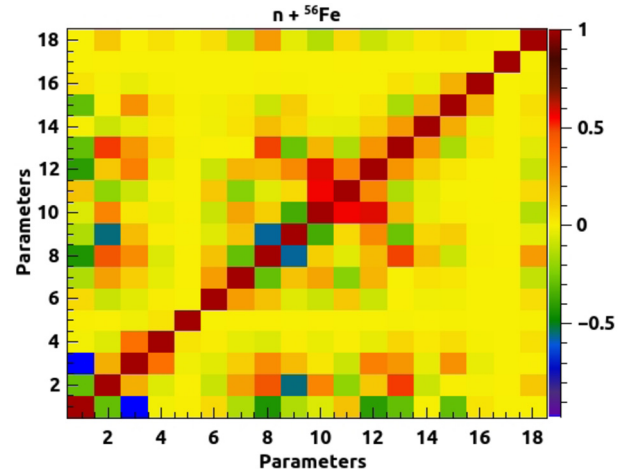


**Fig. 3.** Parameter correlation matrix for  $n+^{56}\text{Fe}$  reaction. Parameters are presented here according to their serial numbers (defined in Table 1).

$r_v$  and  $v_1$  are strongly anti-correlated which is consistent with the relation between  $v_1$  and  $r_v$  i.e.  $v_1 \times r_v^2 = \text{constant}$ . It is also clear from these figures that most of the parameters are anti-correlated (e.g.  $r_v$  and  $a_v$ ,  $d_1$  and  $a_d$ ,  $a_d$  and  $a_v$ ,  $r_d$  and  $a_d$ ,  $r_d$  and  $w_2$  etc.). These observations are consistent with the observations of Duan et al., [6], however they had used a completely different method for calculating the correlation matrix. Some of the parameters also indicate strong positive correlations e.g.  $d_1$  and  $d_2$ ,  $d_1$  and  $d_3$ ,  $a_v$  and  $v_1$ ,  $r_d$  and  $r_{so}$ ,  $a_v$  and  $r_d$  etc. are positively correlated. The updated and initial set of the optical model parameters with the new/old uncertainties associated with them are listed in Table 1. It is clear from the table that the parameter uncertainties depend on the quality and quantity of the experimental data used for the optimization and some of the parameters can be associated with the large uncertainties. It is important to note that the uncertainties for some of the parameters are very low, because the uncertainties for these parameters provided in the ref. [7] which are used as our initial estimate is already very small and a minimum limit on the parameter uncertainties can be set in order to overcome this problem [4]. Also it may be observed from Fig. 8 that the total reaction cross sections obtained through the new set of the optical model parameters are consistent with the experimental data.

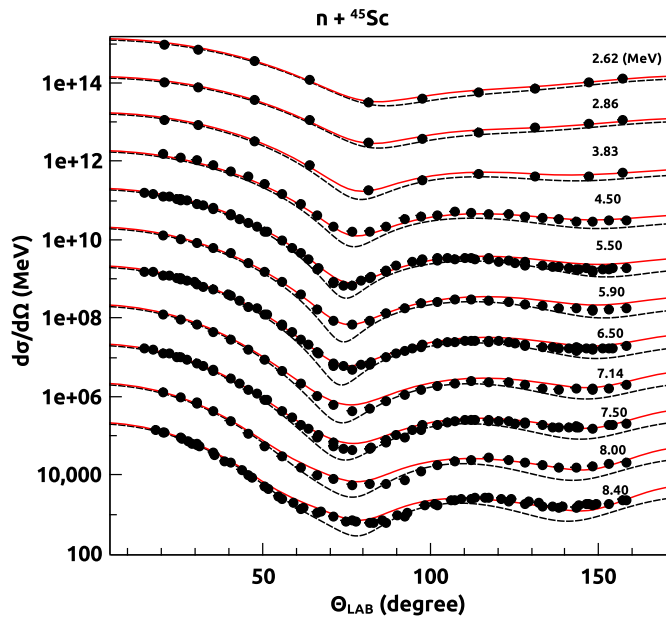


**Fig. 4.** DWBA calculations using updated parameters (in red) relative to the DWBA calculations using initial parameters (in black dotted line) with experimental data (presented in the black dots). Data at different energies have been offset by  $\times 10^3, \times 10^4, \times 10^5, \dots$  etc.

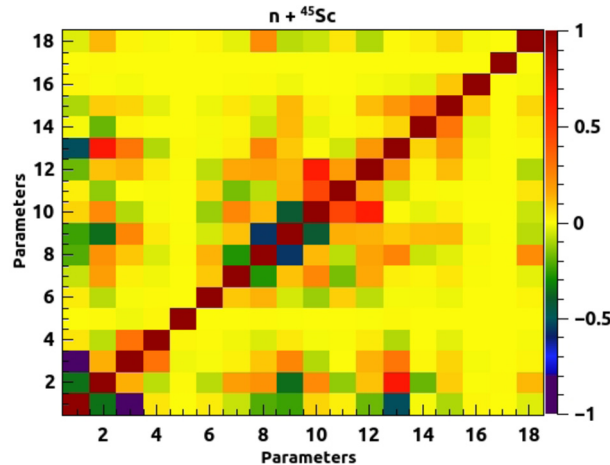


**Fig. 5.** Parameter correlation matrix for  $n + {}^{45}\text{Sc}$  reaction. Parameters are presented here according to their serial numbers (defined in Table 1).

## 6. Conclusions

In this study, we have determined the optical model parameters and their correlation matrices using the Unscented Transform Kalman Filter technique successfully. And the results clearly verify the use of the UTKF for the parameter estimation and uncertainty quantification of the optical model parameters. This study clearly indicates that the optical model parameters are correlated to each other; hence these correlations should be considered while using them to predict the nuclear reaction cross sections. There is no clear reason at this time to believe that why it cannot be used for estimating the other model parameters used for different nuclear reaction models. This method can also be used for the reactions with protons as projectiles, just by including the Coulomb barrier term in the optical model potential. This study is a proof of the concept only and the quality of the estimated optical model parameters and their uncertainties depends on the quality of the

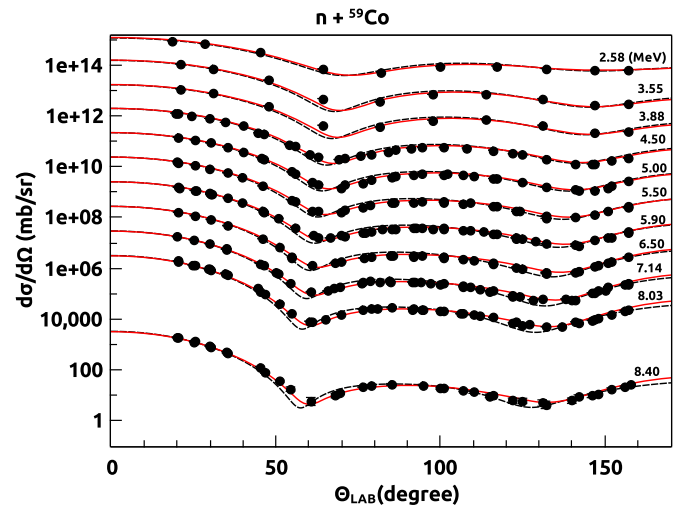


**Fig. 6.** DWBA calculations using updated parameters (in red) relative to the DWBA calculations using initial parameters (in black dotted line) with experimental data (presented in the black dots). Data at different energies have been offset by  $\times 10^3, \times 10^4, \times 10^5, \dots$  etc.

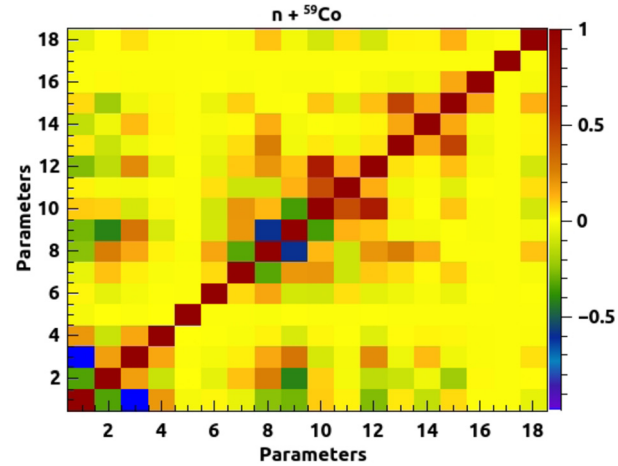


**Fig. 7.** Parameter correlation matrix for  $n + {}^{59}\text{Co}$  reaction. Parameters are presented here according to their serial numbers (defined in Table 1).

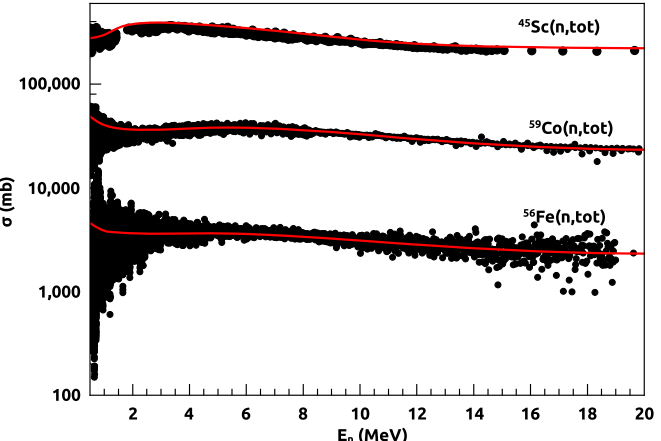


**Fig. 8.** Total reaction cross sections for the  $n + {}^{56}\text{Fe}$ ,  $n + {}^{59}\text{Co}$  and  $n + {}^{45}\text{Sc}$  reactions, by using the optical model parameters obtained through this study (presented as red lines) in comparison to the experimental results from EXFOR data library (presented in the black dots). The cross sections are offset by  $\times 10^1$  and  $\times 10^2$  for the better representation.

initial set of parameters, their uncertainties and the experimental data used for the estimation.

### Declaration of competing interest

The authors declare that they have no known competing financial interests or personal relationships that could have appeared to influence the work reported in this paper.

### Acknowledgements

One of the authors (A. Kumar) thanks to the SERB-DST, Government of India (Sanction No. CRG/2019/000360), IUAC-UGC, Government of India (Sanction No. IUAC/XIII.7/UFR-58310) and UGC-DAE Consortium for Scientific Research (Sanction No. UGC-DAE-CSR-KC/CRS/19/NP03/0913) for the financial support for this work.

### References

- [1] A.J. Koning, D. Rochman, *Ann. Nucl. Energy* 35 (2008) 2024.
- [2] R. Capote, M. Hermana, P. Obložinský, et al., *Nucl. Data Sheets* 110 (2009) 3107–3214.
- [3] A.E. Lovell, F.M. Nunes, J. Sarich, S.M. Wild, *Phys. Rev. C* 95 (2017) 024611.
- [4] M. Herman, *Nucl. Data Sheets* 109 (2008) 2752–2761.
- [5] Yinlu Han, Yongli Xu, Haiying Liang, et al., *Phys. Rev. C* 81 (2010) 024616.
- [6] J. Duan, *Nucl. Data Sheets* 118 (2014) 346–348.
- [7] A.J. Koning, D. Rochman, *Nucl. Data Sheets* 113 (2012) 2841–2934.
- [8] S.J. Julier, J.K. Uhlmann, H.F. Durrant-Whyte, A new approach for filtering nonlinear systems, in: *Proceedings of 1995 American Control Conference, ACC'95*, Seattle, WA, USA, vol. 3, 1995, pp. 1628–1632.
- [9] S.J. Julier, J.K. Uhlmann, A general method for approximating nonlinear transformations of probability distributions, Technical Report, RRG, Department of Engineering Science, University of Oxford, November 1996.
- [10] Simon J. Julier, Jeffrey K. Uhlmann, New extension of the Kalman filter to nonlinear systems, in: *Proc. SPIE 3068, Signal Processing, Sensor Fusion, and Target Recognition VI*, 28 July 1997.
- [11] Dan Simon, *Optimal State Estimation: Kalman, H Infinity, and Nonlinear Approaches*, John Wiley & Sons, 2006, ISBN 0470045337, 9780470045336.
- [12] Eric A. Wan, Rudolph van der Merwe, S. Haykin, The unscented Kalman filter, in: *Kalman Filtering and Neural Networks*, 5.2007, 2001, pp. 221–280.
- [13] A.J. Koning, J.P. Delarocque, *Nucl. Phys. A* 713 (2003) 231–310.
- [14] Adam Attarian, et al., Application of the unscented Kalman filtering to parameter estimation, in: *Mathematical Modeling and Validation in Physiology*, Springer-Verlag Berlin Heidelberg, 2013, pp. 75–85.
- [15] E.A. Wan, R. van der Merwe, The unscented Kalman filter for nonlinear estimation, in: *Proceedings of the IEEE 2000 Adaptive Systems for Signal Processing, Communications, and Control Symposium*, Cat. No. 00EX373, IEEE, 2000, pp. 153–158.
- [16] W.H. Press, S.A. Teukolsky, W.T. Vetterling, B.P. Flannery, *Numerical Recipes in C: The Art of Scientific Computing*, 2nd edition, Cambridge University Press, 1992.
- [17] S.J. Julier, The scaled unscented transformation, in: *Proceedings of the 2002 American Control Conference*, IEEE Cat. No. CH37301, Anchorage, AK, USA, vol. 6, 2002, pp. 4555–4559.
- [18] N. Otuka, et al., *Nucl. Data Sheets* 120 (2014) 272.
- [19] A.J. Koning, S. Hilaire, M.C. Duijvestijn, TALYS 1.0, in: O. Bersillon, F. Gunning, E. Bauge, R. Jacqmin, S. Leray (Eds.), *Proceedings of the International Conference on Nuclear Data for Science and Technology*, April 22–27, 2007, Nice, France, EDP Sciences, 2008, pp. 211–214.
- [20] S.M. El-Kadi, et al., *Nucl. Phys. A* 390 (1982) 509.
- [21] A.P.D. Ramirez, et al., *Phys. Rev. C* 95 (2017) 064605.
- [22] A.B. Smith, P.T. Guenther, *J. Phys. G, Nucl. Part. Phys.* 19 (1993) 655.
- [23] A.B. Smith, P.T. Guenther, R.D. Lawson, *Nucl. Phys. A* 483 (1988) 50.